

A continuum elastic–plastic model for woven-fabric/polymer-matrix composite materials under biaxial stresses

G. Odegard^{a,1}, K. Searles^b, M. Kumosa^{a,*}

^aCenter for Advanced Materials and Structures, Department of Engineering, University of Denver, 2390 S. York, Denver, CO 80208, USA

^bDepartment of Materials Science and Engineering, Oregon Graduate Institute of Science and Technology, PO Box 91000, Portland, OR 97291-1000, USA

Received 13 January 2001; received in revised form 14 August 2001; accepted 25 September 2001

Abstract

In this study a simple continuum model for the macro-mechanical prediction of the elastic–plastic behavior of woven-fabric/polymer-matrix composites has been proposed. This model uses a scalar hardening parameter (which is a function of the current applied stress state) instead of an effective stress-strain relation to determine plastic strain increments. For simplicity, the stresses are expressed as invariants based on the material symmetry. It has been shown, by the use of experimental data for two different woven-fabric/polymer-matrix composite materials, that the newly proposed model accurately describes the non-linear mechanical behavior for different in-plane biaxial stress states ranging from pure shear to pure tension. © 2001 Published by Elsevier Science Ltd. All rights reserved.

Keywords: A. Textile composites; B. Mechanical properties; B. Modeling; B. Plastic deformation

1. Introduction

Woven-fabric composites have received considerable attention in recent years on account of their increased damage tolerance with respect to unidirectional and angle-ply composite laminates and because of the relative ease and low cost of fabrication of composite structures made from woven fabric pre-pregs. A common type of woven-fabric composite used in the aerospace industry is a bi-directional woven carbon-fibre-reinforced polymer (typically epoxy or polyimide). The fabric is woven on a loom and is composed of two sets of interlacing, mutually orthogonal yarns (the longitudinal and width-wise yarns are known as the warp and fill, respectively). The size of each yarn is determined by the number of filaments (or fibers) it contains. The architecture of the fabric is characterized by the interlacing pattern of the warp and weft yarns. The basic geometrical pattern can be characterized by the parameter n which denotes that

the warp yarn is interlaced with every n th fill yarn, and vice versa. For example, Fig. 1 shows an example of a plain woven architecture ($n=2$), and Fig. 2 shows the 8 harness-satin (8HS) woven geometry ($n=8$).

It is well known that woven-fabric/polymer composites exhibit significant non-linear stress/strain behavior when subjected to pure shear or shear-dominated biaxial stresses [1–5]. In many cases, the non-linearity may even be detected upon initial loading of the material and continues until catastrophic failure. This non-linear mechanical response is mostly due to the non-linear constitutive behavior of the polymer matrix, micro-cracking of the matrix material, fiber/matrix interface debonding, and interlaminar delamination. Typically the interlaminar delamination releases a significant amount of energy upon deformation at higher loads and is responsible for a large, irregular change in the stress/strain curve [4,5]. Fig. 3 shows the side view of an 8HS woven graphite/PMR-15 off-axis tensile coupon that has been tested under a large shear-dominated biaxial load. The bulging is due mostly to delaminations that occur between plies and in the crimp area in between perpendicular yarns that relax when the specimen is unloaded. These delaminations start in regions with high stress concentrations, e.g. near intralaminar matrix

* Corresponding author. Tel.: +1-303-871-3807; fax: +1-303-871-4450.

E-mail address: mkumosa@du.edu (M. Kumosa).

¹ Current address: NASA Langley Research Center, M.S. 188 E, Hampton, VA 23681, USA.

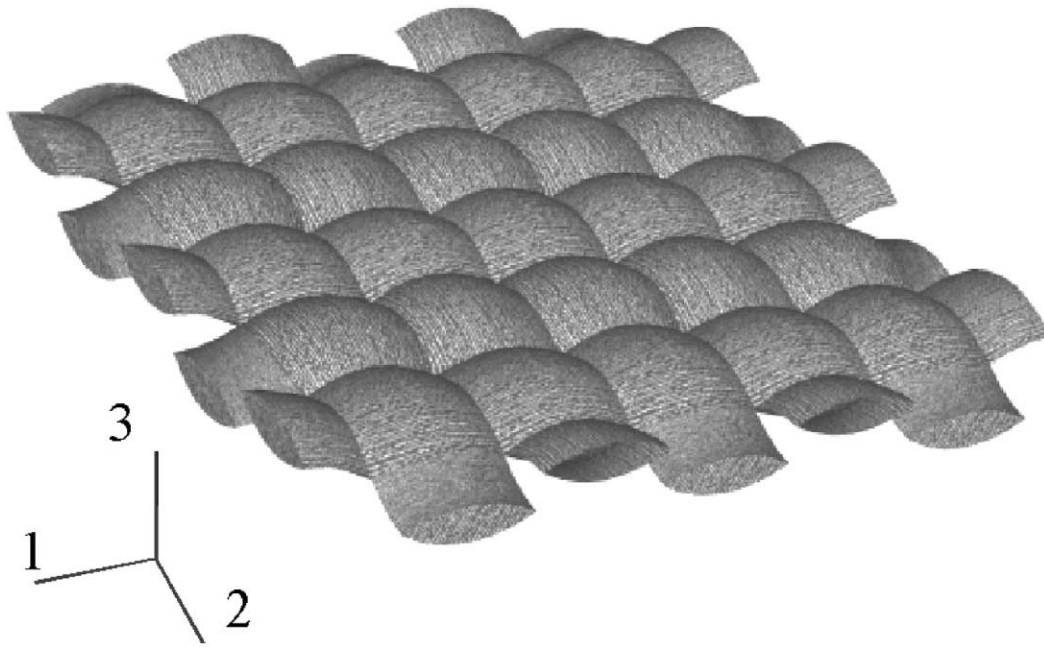


Fig. 1. Plain woven fabric architecture with the material coordinate system indicated.

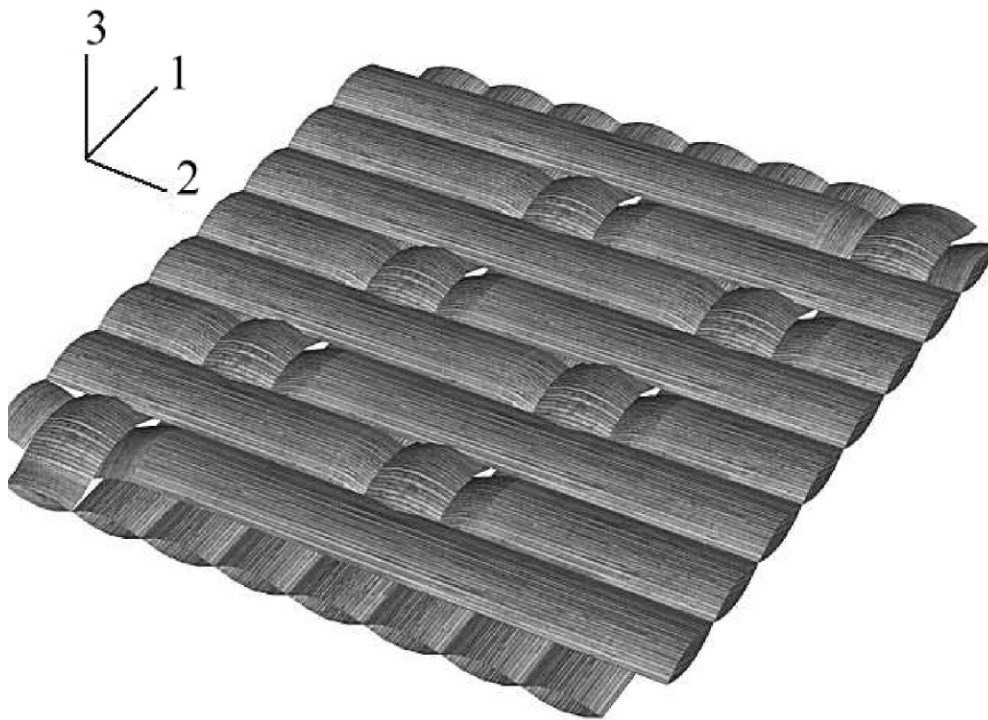


Fig. 2. 8HS woven fabric architecture with the material coordinate system indicated.

cracks, the free edges of the specimen, or crimps of perpendicular yarns.

It has also been shown that woven-fabric/polymer-matrix composites can exhibit noticeable non-linearity when loaded in pure tension or compression along the axes parallel to the fibers [1,3,6]. The primary causes of this non-linearity are micro-cracking of the matrix and fibers. Usually a prominent “knee” in the uniaxial

stress/strain curve can be seen where the transverse cracking of the matrix starts [1]. At much higher loads the composite will fail catastrophically when the fibers begin to fracture or pull out.

These failure modes contribute to a significant amount of macroscopic non-linearity which must be properly characterized and modeled in order to be able to design structures with an acceptable degree of safety.



Fig. 3. Side view of a tested 8HS woven graphite/PMR-15 off-axis specimen showing interlaminar delaminations after unloading.

Due to the large amount of anisotropy and heterogeneity of woven fabric composites on a mesoscopic scale and the tremendously varying modes of micro-damage which depend on the applied stress state (either uniaxial or biaxial, tension or compression), the macroscopic non-linear behavior is strongly dependent upon the applied load path. In order to model this behavior correctly the current stress state and stress history must be considered.

There has been a considerable amount of research performed on the non-linear behavior of woven fabric composites at the meso-mechanical level using numerical [7–10] and analytical approaches [11–15]. These models are concerned with the effects of individual damage mechanisms, such as micro-cracking and non-linear behavior of individual constituents, on the total non-linear response of the composite. These models are very useful for studying the stress fields in composite materials and the contribution of the behavior of the individual constituents on the macroscopic elastic–plastic behavior of the material. However, if the knowledge of this information is not needed or desired, and the only concern is the macro-mechanical behavior of the woven composite material, then the meso-mechanical approach may be overly complicated and time-consuming for the design of a composite structure, especially in the presence of both normal and shear stresses. In this case a continuum model may be more efficient.

Some researchers have developed continuum time-independent plasticity models that can be used to describe the non-linear behavior of woven-fabric/polymer-matrix composite materials. Hill's model [16] was originally developed for anisotropic cold-rolled metals. Vaziri et al. [17] and Odegard et al. [4] used similar approaches as Hill [16] and Sun and Chen [18] for modeling the elastic–plastic behavior of woven graphite/PMR-15 composites. These approaches assume a relationship between an effective stress and effective strain. This is an important assumption in the plasticity of isotropic materials, and has shown some promise in modeling the

plasticity of anisotropic materials. However, Hansen et al. [19] pointed out that it may be an overly restrictive assumption when applied to polymer-matrix composite materials since they exhibit drastically different modes of meso-mechanical failure under different load paths. Hansen et al. [19] proposed an invariant-based flow rule for unidirectional composites which incorporates a scalar hardening parameter that allows the hardening to be determined as a function of the load path, and not an effective stress-strain relationship. The purpose of this study is to extend this non-linear model to woven fabric/polymer composites.

2. Stress and strain tensors

It has been shown experimentally by Fujii et al. [1] that for woven-fabric/polymer-matrix composites loaded to large strains (at least around 0.5%), the 2nd Piola–Kirchhoff stress tensor and the Green–Lagrange strain tensor should be used in order to properly express stress and strain components with respect to the reoriented fabric. At large strains, following failure of the crimp regions and significant interlaminar cracking, the perpendicular yarns in a 2D woven fabric/polymer matrix composite are allowed to rotate with respect to each other towards the direction of the principal stress (Fig. 4). This geometric non-linearity causes a significant change in the stress/strain response of the composite material depending on how the stress and strain tensors are defined [1]. The response can be properly modeled at large strains assuming that the stress and strain components are defined with respect to the original fiber coordinate system in the reoriented state. The symmetric second order 2nd Piola–Kirchhoff stress tensor is defined as:

$$\mathbf{P} = J\mathbf{G}^{-1}\boldsymbol{\sigma}\mathbf{G}^{-T} \quad (1)$$

where J is the Jacobean, \mathbf{G} is the second order deformation gradient tensor, and $\boldsymbol{\sigma}$ is the second order Cauchy

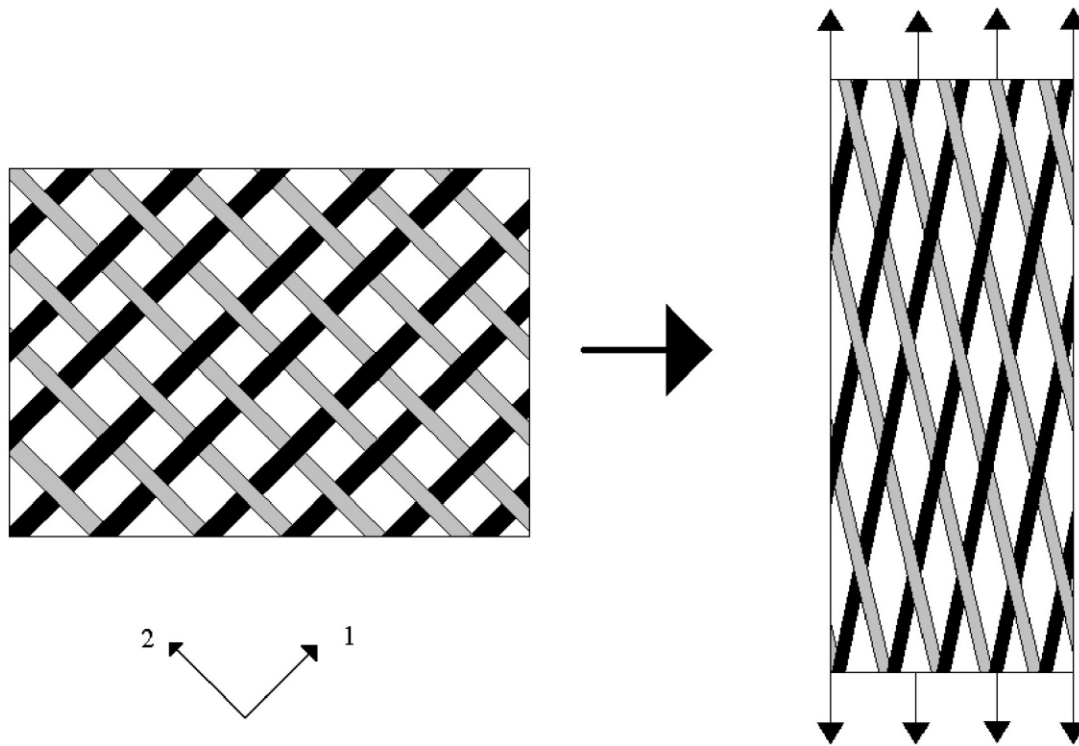


Fig. 4. Deformation of an element of plain woven fabric subjected to large shear strains.

stress tensor. The Green–Lagrange strain tensor is defined as:

$$\varepsilon = \frac{1}{2}(\mathbf{G}^T \mathbf{G} - \mathbf{I}) \quad (2)$$

where \mathbf{I} is the second order identity tensor. When strains are relatively small either the nominal or Cauchy stresses can be used to evaluate the non-linear behavior of fabric composites. However, when strains are large and the displacement gradients are known, the 2nd Piola–Kirchhoff stress tensor should be substituted for the Cauchy stress tensor [1].

3. Elastic deformation

Woven-fabric composites exhibit a significant change in elastic properties as micro-damage propagates when the material is subjected to either static or dynamic deformations. If it is desired to model multiple steps of loading and unloading, then it is important to model the increase in the compliance tensor components as a function of load path. Ju [20] suggested the use of a fourth-order damage tensor to model the macroscopic change in the compliance. The overall compliance tensor of the continuum can be expressed as:

$$\mathbf{S} = \mathbf{S}^\circ[\mathbf{I} + \mathbf{D}] \quad (3)$$

where \mathbf{S}° is the fourth order undamaged compliance tensor, \mathbf{I} is the fourth order identity tensor, and \mathbf{D} is the fourth order damage tensor. Each component of the damage tensor is zero for an undamaged material and should increase as a function of propagating micro-damage. In general, the damage will affect the compliance tensor differently for states of tension and compression due to different micro-damage modes (e.g. matrix cracking in tension vs. fiber kinking in compression). Therefore, the normal and interaction components of the damage tensor (e.g. D_{11} , D_{22} , D_{12} , and D_{21}) should have two separate values associated with tensile and compressive stresses. For plane stress, the total compliance tensor components can be assumed to be (in contracted notation where i, j , and $k = 1, 2, \dots, 6$):

$$S_{ij} = \begin{bmatrix} S_{11} & S_{12} & 0 \\ S_{21} & S_{22} & 0 \\ 0 & 0 & S_{66} \end{bmatrix} \quad (4)$$

The compliance tensor of the undamaged woven fabric composite is:

$$S_{ij}^\circ = \begin{bmatrix} S_{11}^\circ & S_{12}^\circ & 0 \\ S_{12}^\circ & S_{11}^\circ & 0 \\ 0 & 0 & S_{66}^\circ \end{bmatrix} \quad (5)$$

The individual components of the damage tensor may be described by the following functions:

$$D_{ij} = D_{ij}(\alpha_1, \alpha_2, \dots, \alpha_\beta) \tag{6}$$

where $D_{16} = D_{61} = D_{26} = D_{62} = 0$ [from Eqs. (3)–(5)] and each α argument is an individual state variable ($\beta = 1, 2, \dots$, total number of state variables) that can be used to describe the current damage state, such as the maximum attained stress components along each principal material axis in tension and compression, total number of fatigue cycles, fatigue stress ratio, etc. Eq. (6) represents a continuum damage evolution law of the woven-fabric composite material.

4. Yield function

When considering the most generalized case of a composite that behaves differently (as far as yielding and plastic deformation) along different material axes in both tension and compression, a yield function must be used that has the proper yield surface shape in stress space that will reflect this behavior. Tsai and Wu [21] developed a generalized yield function for composite materials using a continuum approach:

$$\Phi(\sigma_k) = \phi(\sigma_k) - \underline{\phi} = 0 \tag{7}$$

where ϕ is the largest recorded value of $\phi(\sigma_k)$ (for initial yield is taken as unity), σ_k is the stress tensor, and

$$\phi(\sigma_k) = F_i \sigma_i + F_{ij} \sigma_i \sigma_j \tag{8}$$

where F_i and F_{ij} are strength tensors of the second and fourth rank, respectively. Eqs. (7) and (8) describe the shape of the yield surface in stress space. The linear and quadratic stress terms allow tensile and compressive values of strength to be evaluated separately. In the case of a 2D woven-fabric fiber architecture the two principal fiber axes are parallel to the 1 and 2 axes (see Figs. 1 and 2) and it may be assumed that the strength and plastic flow properties along these two principal axes are the same. Therefore, Eq. (8) may be expanded by index summation and then reduced to:

$$\begin{aligned} \phi(\sigma_k) = & F_1(\sigma_1 + \sigma_2) + F_3(\sigma_3) + F_{11}(\sigma_1^2 + \sigma_2^2) \\ & + 2F_{12}(\sigma_1\sigma_2) + 2F_{13}(\sigma_1\sigma_3 + \sigma_2\sigma_3) \\ & + F_{33}\sigma_3^2 + F_{44}(\sigma_4^2 + \sigma_5^2) + F_{66}\sigma_6^2 \end{aligned} \tag{9}$$

The components of the strength tensors are:

$$\begin{aligned} F_{11} = \frac{1}{XX'}; \quad F_1 = \frac{1}{X} - \frac{1}{X'}; \quad F_{33} = \frac{1}{ZZ'}; \\ F_3 = \frac{1}{Z} - \frac{1}{Z'}; \quad F_{44} = \frac{1}{Q^2}; \quad F_{66} = \frac{1}{S^2} \end{aligned} \tag{10}$$

where X and X' are the yield points on the yield surface along the 1 and 2 axes of the woven-fabric composite in

tension and compression, respectively. Z and Z' are the yield points on the 3 axes in tension and compression, respectively. Q and S are the yield points for shear in the 2,3 and 1,3 plane and the 1,2 plane of the composite material, respectively. The strength tensor components F_{12} and F_{13} are biaxial interaction parameters which are sensitive to the particular material considered. They should be determined experimentally for any given composite using a test that subjects the material to a multi-axial stress state. In the case of plane stress in the 1,2 plane Eq. (9) becomes:

$$\begin{aligned} \phi(\sigma_k) = & F_1(\sigma_1 + \sigma_2) + F_{11}(\sigma_1^2 + \sigma_2^2) + 2F_{12}(\sigma_1\sigma_2) \\ & + F_{66}\sigma_6^2 \end{aligned} \tag{11}$$

The material behavior is defined by:

- $\Phi < 0$: elastic
- $\Phi = 0$: the stress state is on the yield surface, plastic deformation occurring as loading progresses
- $\Phi > 0$: inaccessible state

It is assumed that proportional hardening takes place, unless kinetic terms are inserted into Eqs. (7) and (8). For polymer matrix composites, proportional hardening is usually adequate to describe the elastic-plastic material behavior.

5. Flow rule

A general form of the associated flow rule is [22]:

$$d\varepsilon_i^p = g(\sigma_i) \left(\frac{\partial \Phi}{\partial \sigma_j} d\sigma_j \right) \frac{\partial \Phi}{\partial \sigma_i} \tag{12}$$

where $d\varepsilon_i^p$ is the plastic strain increment tensor and $g(\sigma_i)$ is the scalar hardening parameter. Plastic flow occurs when:

$$\frac{\partial \Phi(\sigma_k)}{\partial \sigma_j} d\sigma_j > 0 \quad \text{and} \quad \Phi(\sigma_k) = 0 \tag{13}$$

The scalar hardening parameter, $g(\sigma_i)$, is a scalar function of a second-order tensor. It serves as a factor that describes the plastic hardening of the composite as a function of applied stress. It has been shown [19] that $g(\sigma_i)$ can be put into a form in which its value depends on the location of the stress state on the yield surface. The form of $g(\sigma_i)$ may be restricted by considering invariance properties of the composite material so that it remains unchanged for arbitrary symmetry operations characteristic of the orientation of the fibers. The five stress invariants used by Hansen et al. [19] for a uni-directional composite were [23]:

$$\begin{aligned} \gamma_1 = \sigma_1; \quad \gamma_2 = \sigma_2 + \sigma_3; \quad \gamma_3 = \sigma_2^2 + \sigma_3^2 + 2\sigma_4^2; \\ \gamma_4 = \sigma_6^2 + \sigma_5^2; \quad \gamma_5 = \sigma_2\sigma_6^2 + \sigma_3\sigma_5^2 + 2\sigma_6\sigma_5\sigma_4 \end{aligned} \tag{14}$$

The eight stress invariants for a 2D bi-directional woven composite (assuming ditetragonal-dipyramidal type symmetry) are [23]:

$$\begin{aligned} a_1 &= \sigma_1 + \sigma_2; a_2 = \sigma_3; a_3 = \sigma_4^2 + \sigma_5^2; a_4 = \sigma_6^2; a_5 = \sigma_1\sigma_2 \\ a_6 &= \sigma_4\sigma_5\sigma_6; a_7 = \sigma_1\sigma_4^2 + \sigma_2\sigma_5^2; a_8 = \sigma_4^2\sigma_5^2 \end{aligned} \quad (15)$$

Ideally, stress invariants a_1 , a_2 , a_5 , and a_7 should cause different non-linear behavior if their signs are changed. Therefore, in general, the effect of the negative values should be considered in the formulation of the scalar hardening parameter. $g(\sigma_i)$ may be put into the form:

$$g(\sigma_i) = g(a_1, a_2, a_3, a_4, a_5, a_6, a_7, a_8) \quad (16)$$

In the case of plane stress, Eq. (16) can be reduced to:

$$g(\sigma_i) = g(a_1, a_4, a_5) \quad (17)$$

Eq. (17) can be more conveniently expressed as [19]:

$$g(\sigma_i) = \frac{a_1}{a_1^*} g_1(a_1) + \frac{a_4}{a_4^*} g_2(a_4) + \frac{a_5}{a_5^*} g_3(a_5) \quad (18)$$

where the superscript * indicates values of the invariants at the current yield surface assuming a uniaxial invariant stress state (the sign of which depends on the sign of the invariant), and $g_n(a_m)$ is a function determined empirically for each individual invariant. Hansen et al. [19], Odegard and Kumosa [24] and Odegard et al. [25] showed that a linear equation for each $g_n(a_m)$ will result in a $g(\sigma_i)$ that satisfactorily matches the experimental stress-strain data for a multi-axial stress state in uni-directional composites. For example:

$$g_1(a_1) = \begin{cases} A_1 a_1 + A_2 & \text{if } a_1 \geq 0 \\ A_3 a_1 + A_4 & \text{if } a_1 < 0 \end{cases} \quad (19)$$

$$g_2(a_4) = A_5 a_4 + A_6 \quad (20)$$

$$g_3(a_5) = \begin{cases} A_7 a_5 + A_8 & \text{if } a_5 \geq 0 \\ A_9 a_5 + A_{10} & \text{if } a_5 < 0 \end{cases} \quad (21)$$

where $A_1 \dots A_{10}$ are constants that are determined experimentally (by using uniaxial or biaxial mechanical tests). A similar approach can be used in the more generalized case of a 3D stress state.

The total incremental strain is the sum of the elastic and plastic strain increments:

$$d\epsilon_i^t = d\epsilon_i^e + d\epsilon_i^p \quad (22)$$

where the superscripts t , e , and p denote total, elastic, and plastic strains, respectively. The plastic strain

increment is given in Eq. (12) and the elastic strain increment is a function of the applied stress and the compliance tensor given in Eq. (3):

$$d\epsilon_i^e = S_{ij} d\sigma_j + dS_{ij} \sigma_j \quad (23)$$

Generally, in woven-fabric-reinforced polymer composites, the elastic strain increment is much smaller than the plastic strain increment when loaded to relatively large strains. The influence of the change in the compliance tensor due to damage on the stress/strain curve is small compared to the influence of the plastic deformation. Therefore, for simplicity, it may be assumed that under plastic deformation ($\Phi=0$) the compliance tensor remains constant and the second term on the right hand side of Eq. (23) is zero. When the material is starting to unload and is in the elastic range ($\Phi < 0$), the compliance tensor may be modified based on Eq. (6) and dS_{ij} is briefly non-zero. Once the compliance is updated, then the second term on the right hand side of Eq. (23) is once again zero until another change in compliance occurs.

6. Experimental characterization

In general, the complete experimental determination of the material parameters $F_1, F_{11}, F_3, F_{33}, F_{44}, F_{66}, F_{12}, F_{13}, A_1-A_{10}$, and D_{ij} is not simple. The parameters are not all necessary for each particular loading case. Depending on the mechanical behavior of interest, assumptions can be made to reduce the number of total parameters. The model then reduces to a relatively simple analysis compared to the micro-mechanics approach.

For example, the following series of mechanical tests could be used to characterize the parameters for a composite material subjected to a plane stress state and assuming that the properties are the same along the 1 and 2 axes:

- X, X' , and A_1-A_4 can be determined by applying tensile and compressive uniaxial loads (so that $a_1 \neq 0$ and $a_5 = 0$) along a material axis that is parallel to one set of fibers, thus determining F_1 and F_{11} using Eq. (10) and $g_1(a_1)$ using Eqs. (18) and (19). This step can be easily performed using torsional tubes or tensile/compression specimens.
- S, F_{66}, A_5 , and A_6 can be determined by subjecting a specimen to pure in-plane shear using Eqs. (10), (18) and (20). D_{66} can also be determined based on the assumptions in Eq. (6). This can be accomplished with a torsional test of a torsional tube.
- F_{12}, A_9 and A_{10} can be determined with a biaxial test so that $a_1 = 0$ and $a_5 < 0$, thus $\sigma_1 = -\sigma_2$. This can be accomplished with a picture-frame type test [26] using Eqs. (10), (11), (18) and (21).

- A_7 and A_8 must be determined using a multi-axial test where $a_1 > 0$, $a_5 > 0$, and $a_4 > \text{or} = 0$, thus $\sigma_1 = 0$ and $\sigma_2 > 0$, using Eqs. (18)–(21). Any biaxial mechanical test could be used for this.
- D_{11} , D_{22} , D_{12} , and D_{21} can be determined using the assumptions in Eqs. (6) and the change in the compliance constants observed upon unloading and/or reloading after uniaxial loading along the 1 or 2 axes using Eq. (3)–(5).

If it is assumed that the behavior in tension and compression is the same, then $F_1 = 0$, $A_1 = A_3$, $A_2 = A_4$, $A_7 = A_9$ and $A_8 = A_{10}$ and the same method as above can be used to determine F_{11} , F_{66} , A_1 , A_2 , A_5 , A_6 , A_7 and A_8 (the final step is unnecessary). If it is further assumed that non-linear deformation and damage occurs only in shear (no non-linear deformation parallel to the fibers), then A_1 , A_2 , A_7 and A_8 , can be set to zero. Once all of the necessary constants have been determined, then the elastic-plastic and damage behavior of the material may be predicted for any biaxial loading condition using the necessary assumptions.

7. Experiments

Two sets of experimental data on two different woven-fabric/polymer-matrix composite materials have been employed to demonstrate the use of this elastic-plastic model [1, 4]. The scalar hardening parameters for the two composite systems have been determined and

used to predict the stress-strain behavior for different biaxial stress states.

7.1. Plain woven glass/polyester laminate

The experimental data from Fujii et al. [1] was used to determine a scalar hardening parameter for plain woven MG-252/Polylyte FG-284 torsional tube specimens subjected to biaxial loading conditions. The resulting elastic-plastic model and the averaged experimental stress/strain curves (2nd Piola–Kirchhoff stress and Green–Lagrange strain) from Fujii et al. [1] are shown in Figs. 5 and 6 for the response in tension parallel to the fibers and in shear, respectively, for $r = 0/1$, $1/0$, $1/1$, $3/1$, and $7/1$ ($r = \text{tension parallel to fibers/shear}$). The scalar hardening parameter was determined using the pure tension ($r = 1/0$) and pure shear tests ($r = 0/1$) assuming plane stress and that the behavior in tension and compression is the same for this material. Therefore, in this case, $F_1 = 0$, $A_2 = A_4$, $A_7 = A_9$ and $A_8 = A_{10}$. A_7 , A_8 and F_{12} were assumed to be zero for convenience since $\sigma_2 = 0$ for every uniaxial and biaxial test. It was determined that A_1 could be set to zero and $g_1(a_1)$ accurately described by A_2 . The remaining parameters (F_{11} , F_{66} , A_2 , A_5 and A_6) used in the model were determined by fitting the elastic-plastic model to the experimental data (see Table 1 for the values of the parameters). It can be seen that for all of the biaxial loading conditions the elastic-plastic model predicts the non-linear behavior of the composite with an acceptable degree of accuracy.

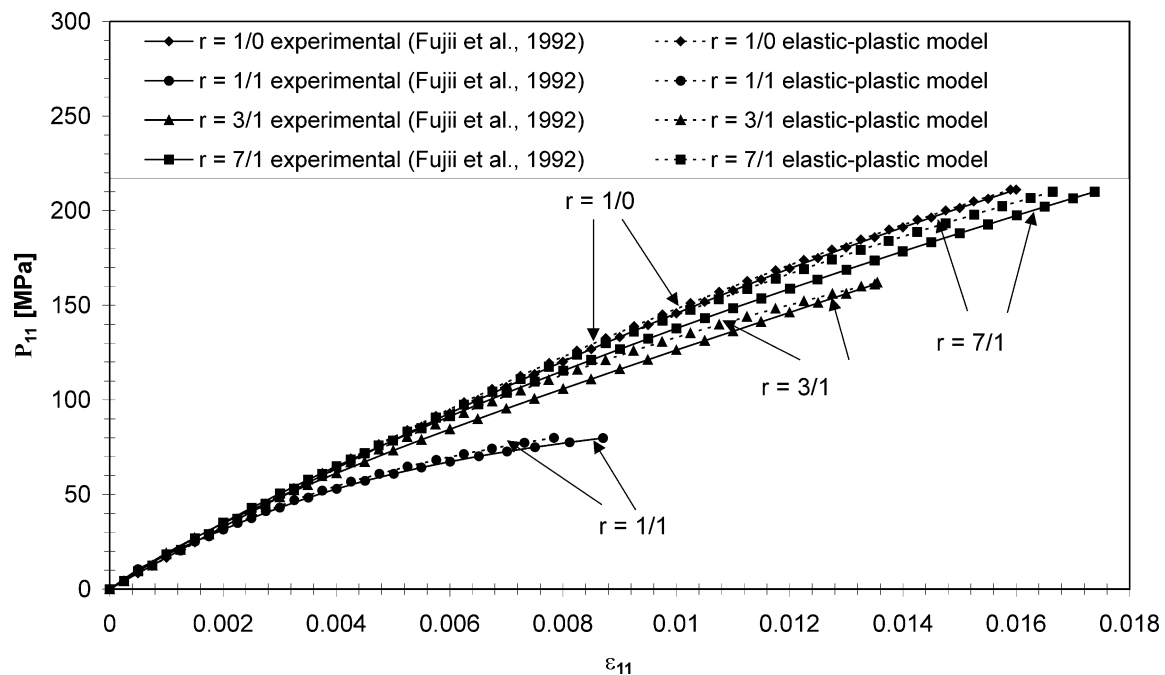


Fig. 5. Stress/strain diagram (parallel to one set of fibers) of the glass/polyester composite showing experimental and modeled responses for four biaxial ratios ($r = \text{normal stress parallel to fibers/shear stress}$).

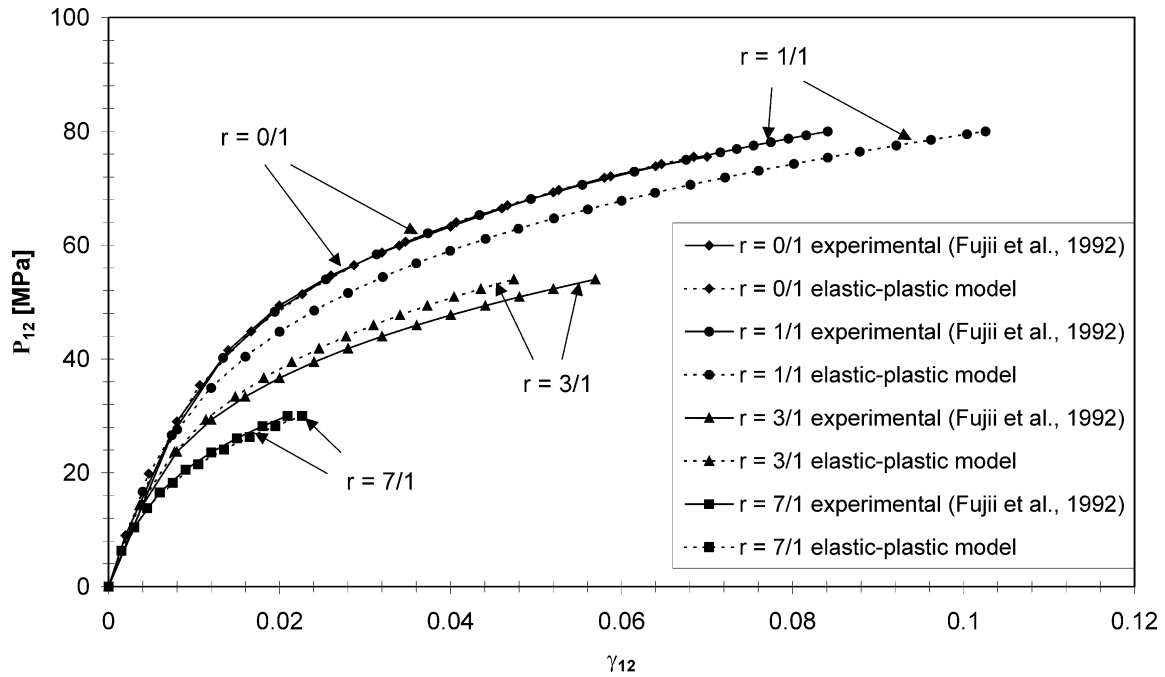


Fig. 6. Shear stress–shear strain diagram of the glass/polyester composite showing experimental and modeled responses for four biaxial ratios (r = normal stress parallel to fibers/shear stress).

7.2. 8HS woven graphite/polyimide laminate

The elastic–plastic behavior of the 8HS woven T650-35/PMR-15 composite material investigated by Odegard et al. [4] and Searles et al. [5] using off-axis tensile tests was determined using the proposed elastic–plastic model. The off-axis experiments were performed at 15, 30, and 45° with respect to the loading axis. Due to strain gage debonding occurring at loads approximately 10% below failure, only approximately 90% of the stress/strain curves were available. Since the large deformation effect on the stress and strain determination was only noticeable

at large strains [1] the nominal stress/strain approach was used to model the non-linear behavior of the graphite/polyimide fabric material using the proposed model.

Fig. 7 shows the experimental axial stress/strain response of the off-axis tensile test specimens, the linear-elastic response determined from the initial slopes, and the response computed from the elastic–plastic model using the scalar hardening parameter. It was assumed that a plane stress state existed, the properties were identical in tension and compression, and only shear stress components (relative to the fiber directions) cause non-linear behavior. Therefore, in addition to the assumptions made for the glass/polyester composite, it is also assumed that $A_2=0$ and $F_{12} \neq 0$ (since σ_1 and $\sigma_2 \neq 0$ the interaction parameter F_{12} is necessary). For this example, the interaction parameter, F_{12} , was assumed to be [27]:

$$F_{12} = \frac{-0.5}{X^2} \tag{24}$$

Table 1
Elastic constants and elastic–plastic parameters used in the analysis of the glass/polyester and graphite/polyimide woven fabric composite systems

Parameter	Plain woven glass-polyester matrix	8HS woven graphite-polyimide matrix
E_{11}	16.7 GPa	79.0 GPa
G_{12}	4.7 GPa	6.1 GPa
ν_{12}	0.15	0.15
F_{11}	0.004 MPa ⁻²	0.0004 MPa ⁻²
F_{66}	0.063 MPa ⁻²	0.004 MPa ⁻²
F_{12}	0.0 MPa ⁻²	-0.0002 MPa ⁻²
A_1	0.0 MPa	0.0 MPa
A_2	1.3×10^{-5} MPa	0.0 MPa
A_5	1.85×10^{-9} MPa ⁻¹	2.0×10^{-8} MPa ⁻¹
A_6	5.3×10^{-6} MPa	1.7×10^{-4} MPa
A_7	0.0 MPa ⁻¹	0.0 MPa ⁻¹
A_8	0.0 MPa	0.0 MPa

A scalar hardening parameter was determined that describes the elastic–plastic behavior of the material under the three different biaxial stress states (see Table 1 for the values of the parameters). In Fig. 7 it is clear that the elastic–plastic model fits the experimental data extremely well relative to the assumption of linear-elasticity for each biaxial stress condition. It can be expected that if the full stress/strain curves were available for this material (up to failure) and the 2nd Piola–Kirchhoff stresses and Green–Lagrange strains were used, then the proposed model would provide the same agreement with the experiment.

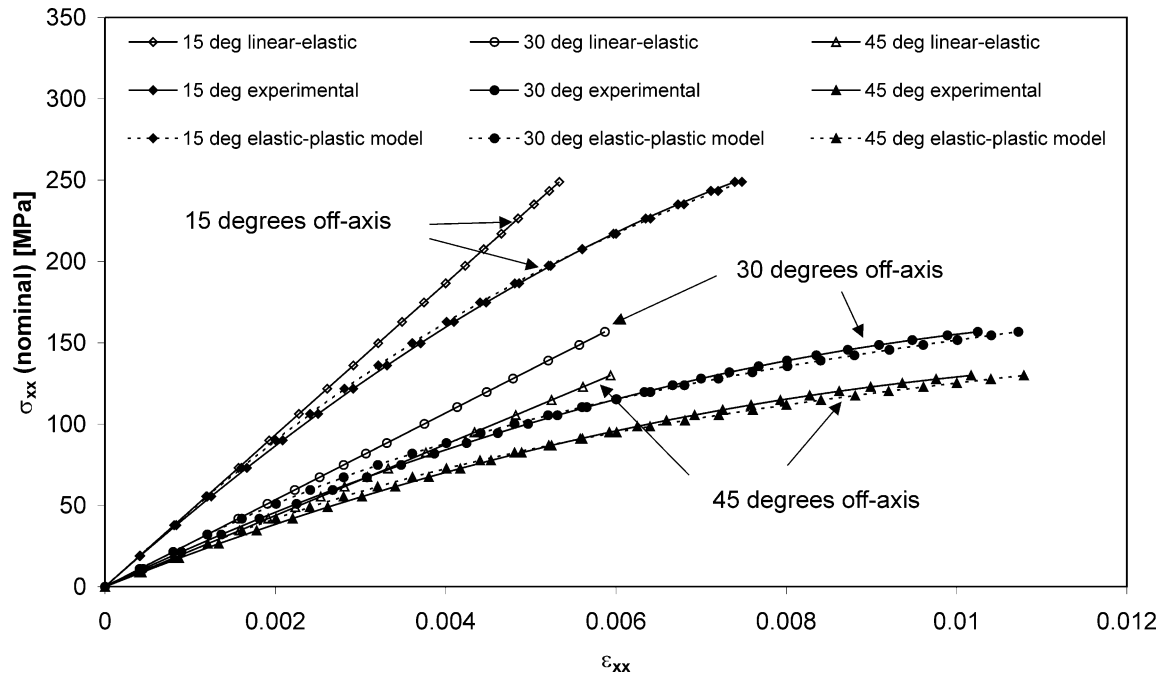


Fig. 7. Axial stress/strain diagram of the graphite/polyimide composite for three off-axis loading angles (rotation of the material coordinates with respect to the loading axis).

8. Conclusion

The non-linear mechanical response of woven-fabric/polymer-matrix composites can be significant under uniaxial or biaxial loading conditions, and should be modeled during the design of a composite structure that must withstand large uniaxial or biaxial stresses. If the details of the meso-mechanical failures are not known or are not considered important for the application, then a continuum elastic-plastic and damage model can be used to predict the mechanical behavior of the composite.

In this study a simple continuum model for the macro-mechanical prediction of the elastic-plastic behavior of woven-fabric/polymer-matrix composites has been proposed. This model uses a scalar hardening parameter (which is a function of the current applied stress state) instead of an effective stress/strain relation to determine plastic strain increments. It has been shown, using experimental data of two different woven fabric/polymer matrix composite materials, that the elastic-plastic model accurately describes the non-linear mechanical behavior for different biaxial stress states.

Acknowledgements

This research was supported by the National Science Foundation under grant CMS-9696169 and the Air Force Office of Scientific Research and the NASA Glenn Research Center under joint grant F49620-00-1-0159.

References

- [1] Fujii T, Amijima S, Lin F, Sagami T. Study on strength and nonlinear stress-strain response of plain woven glass fiber laminate under biaxial loadings. *Journal of Composite Materials* 1992;26(17):2493–510.
- [2] Tanaka T, Fujii T, Kamada M. Effect of loading path on the stress-strain relation and progressive damage of a polymer-matrix composite under tension/torsion biaxial loading. *Journal of Thermoplastic Composite Materials* 1996;9:329–41.
- [3] Tanaka T, Fujii T, Ishikawa A. Damage progression and failure of glass fabric composites subjected to tension/tension and tension/shear combined stresses. *Journal of Thermoplastic Composite Materials* 1998;11:82–96.
- [4] Odegard G, Searles K, Kumosa M. Non-linear analysis of woven fabric-reinforced graphite/PMR-15 composites under shear-dominated biaxial loads. *Mechanics of Composite Materials and Structures* 2000;7(2):129–52.
- [5] Searles K, Odegard G, Kumosa M, Castelli M. Failure investigation of graphite/polyimide fabric composites at room and elevated temperatures. *Journal of Composite Materials* 1999;33(22):2038–79.
- [6] Gao F, Boniface L, Ogin SL, Smith PA, Greaves RP. Damage accumulation in woven-fabric CFRP laminates under tensile loading: Part 1. Observations of damage accumulations. *Composites Science and Technology* 1999;59:123–36.
- [7] Mirzadeh F, Reifsnider KL. Micro-Deformations in C3000/PMR-15 woven composite. *Journal of Composite Materials* 1992;26(2):185–205.
- [8] Blacketter DM, Walrath DE, Hansen AC. Modeling damage in a plain weave fabric-reinforced composite material. *Journal of Composites Technology and Research* 1993;15(2):136–42.
- [9] Naik RA. Failure analysis of woven and braided fabric reinforced composites. *Journal of Composite Materials* 1995;29(17):2334–63.
- [10] Tabiei A, Jiang Y. Woven fabric composite material model with material nonlinearity for nonlinear finite element simulation. *International Journal of Solids and Structures* 1999;36:2757–71.

- [11] Naik NK, Ganesh VK. Failure behavior of plain weave fabric laminates under on-axis uniaxial tensile loading: II. analytical predictions. *Journal of Composite Materials* 1996;30(16):1779–822.
- [12] Ishikawa T, Chou TW. Nonlinear behavior of woven fabric composites. *Journal of Composite Materials* 1983;17:399–413.
- [13] Naik NK, Ganesh VK. Failure behavior of plain weave fabric laminates under in-plane shear loading. *Journal of Composites Technology and Research* 1994;16(1):3–20.
- [14] Gao F, Boniface L, Ogin SL, Smith PA, Greaves RP. Damage accumulation in woven-fabric CFRP laminates under tensile loading: Part 2. Modeling the E=effect of damage on macro-mechanical properties. *Composites Science and Technology* 1999; 59:137–45.
- [15] Scida D, Aboura Z, Benzeggagh ML, Bocherens E. A Micro-mechanics model for 3D elasticity and failure of woven-fibre composite materials. *Composites Science and Technology* 1999; 59:505–17.
- [16] Hill R. A theory of the yielding and plastic flow of anisotropic metals. *Proceedings of the Royal Society of London* 1948;A(193): 281–97.
- [17] Vaziri R, Olson MD, Anderson DL. A plasticity-based constitutive model for fibre-reinforced composite laminates. *Journal of Composite Materials* 1991;25:512–35.
- [18] Sun CT, Chen JL. A simple flow rule for characterizing nonlinear behavior of fiber composites. *Journal of Composite Materials* 1989;23(10):1009–20.
- [19] Hansen AC, Blackketter DM, Walrath DE. An invariant-based flow rule for anisotropic plasticity applied to composite materials. *Journal of Applied Mechanics* 1991;58(4):881–8.
- [20] Ju W. Isotropic and anisotropic damage variables in continuum damage mechanics. *Journal of Engineering Mechanics* 1990; 116(12):2764–70.
- [21] Tsai SW, Wu EM. A general theory of strength for anisotropic materials. *Journal of Composite Materials* 1971;5:512–35.
- [22] Mendelson A. *Plasticity: theory and application*. New York: Macmillan, 1968.
- [23] Spencer AJM. *Theory of invariants*. Continuum physics volume I. New York: Academic Press, 1971.
- [24] Odegard G, Kumosa M. Determination of shear strength of unidirectional composites materials with the Iosipescu and 10° off-axis shear Tests. *Composites Science and Technology* 2000;60: 2917–43.
- [25] Odegard G, Kumosa M. Elastic–plastic and failure properties of a unidirectional carbon/PMR-15 composite at room and elevated temperatures. *Composites Science and Technology* 2000;60:2979–88.
- [26] Kennedy JM, Barnett TR, Farley GL. Experimental and analytical evaluation of a biaxial test for determining in-plane shear properties of composites. *SAMPE Quarterly* 1992;24(1):28–37.
- [27] Odegard G, Searles K, Kumosa M. Critical examination of the Iosipescu shear test as applied to 0° unidirectional composite materials. *Mechanics of Composite Materials and Structures* 1999;6(3):229–56.